



[J Endocr Soc](#). 2020 Oct 1; 4(10): bvaa104.

PMCID: PMC7485795

Published online 2020 Jul 27. doi: [10.1210/jendso/bvaa104](https://doi.org/10.1210/jendso/bvaa104)

Multisystem Progeroid Syndrome With Lipodystrophy, Cardiomyopathy, and Nephropathy Due to an *LMNA* p.R349W Variant

[Iram Hussain](#),¹ [Ruilin Raelene Jin](#),² [Howard B A Baum](#),³ [Jerry R Greenfield](#),⁴ [Sophie Devery](#),² [Chao Xing](#),⁵ [Robert A Hegele](#),⁶ [Barbara G Carranza-Leon](#),³ [Macrae F Linton](#),⁷ [Frank Vuitch](#),⁸ [Kathy H C Wu](#),² [Débora Rossi Precioso](#),⁹ [Junko Oshima](#),¹⁰ [Anil K Agarwal](#),¹¹ and [Abhimanyu Garg](#)¹¹

¹ Division of Endocrinology, Department of Internal Medicine, UT Southwestern Medical Center, Dallas, Texas, USA

² Department of Clinical Genomics, St Vincent's Hospital Sydney, Darlinghurst, NSW, Australia

³ Division of Diabetes, Endocrinology, and Metabolism, Vanderbilt University Medical Center, Nashville, Tennessee, USA

⁴ Department of Endocrinology, St Vincent's Hospital Sydney, Darlinghurst, NSW, Australia

⁵ Eugene McDermott Center for Human Growth and Development, Department of Population and Data Sciences, and Department of Bioinformatics, UT Southwestern Medical Center, Dallas, Texas, USA

⁶ Department of Medicine, Western University, London, Ontario, Canada

⁷ Division of Cardiovascular Medicine, Department of Medicine, Vanderbilt University Medical Center, Nashville, Tennessee, USA

⁸ Department of Pathology, UT Southwestern Medical Center, Dallas, Texas, USA

⁹ Physician Sarah Network of Rehabilitation Hospitals (Unit Belo Horizonte), Internal Medicine, Preoperative Outpatient Clinic, Osteometabolism, Belo Horizonte, Brazil

¹⁰ Department of Pathology, University of Washington, Seattle, Washington, USA

¹¹ Division of Nutrition and Metabolic Diseases, Department of Internal Medicine, and Center for Human Nutrition, UT Southwestern Medical Center, Dallas, Texas, USA

Abhimanyu Garg: abhimanyu.garg@utsouthwestern.edu

Correspondence: Abhimanyu Garg, MD, Division of Nutrition and Metabolic Diseases, Department of Internal Medicine and the Center for Human Nutrition, UT Southwestern Medical Center, 5323 Harry Hines Boulevard, Dallas, TX 75390-8537. Email: abhimanyu.garg@utsouthwestern.edu.

Received 2020 Mar 2; Accepted 2020 Jul 21.

[Copyright](#) © Endocrine Society 2020.

This is an Open Access article distributed under the terms of the Creative Commons Attribution-NonCommercial-NoDerivs licence (<http://creativecommons.org/licenses/by-nc-nd/4.0/>), which permits non-commercial reproduction and distribution of the work, in any medium, provided the original work is not altered or transformed in any way, and that the work is properly cited. For commercial re-use, please contact journals.permissions@oup.com

Abstract

Background

Pathogenic variants in lamin A/C (*LMNA*) cause a variety of progeroid disorders including Hutchinson-Gilford progeria syndrome, mandibuloacral dysplasia, and atypical progeroid syndrome. Six families with 11 patients harboring a pathogenic heterozygous *LMNA* c.1045C>T; p.R349W variant have been previously reported to have partial lipodystrophy, cardiomyopathy, and focal segmental glomerulosclerosis (FSGS), suggesting a distinct progeroid syndrome.

Methods

We report 6 new patients with a heterozygous *LMNA* p.R349W variant and review the phenotype of previously reported patients to define their unique characteristics. We also performed functional studies on the skin fibroblasts of a patient to seek the underlying mechanisms of various clinical manifestations.

Results

Of the total 17 patients, all 14 adults with the heterozygous *LMNA* p.R349W variant had peculiar lipodystrophy affecting the face, extremities, palms, and soles with variable gain of subcutaneous truncal fat. All of them had proteinuric nephropathy with FSGS documented in 7 of them. Ten developed cardiomyopathy, and 2 of them died early at ages 33 and 45 years. Other common features included premature graying, alopecia, high-pitched voice, micrognathia, hearing loss, and scoliosis. Metabolic complications, including diabetes mellitus, hypertriglyceridemia, and hepatomegaly, were highly prevalent. This variant did not show any abnormal splicing, and no abnormal nuclear morphology was noted in the affected fibroblasts.

Conclusions

The heterozygous *LMNA* p.R349W variant in affected individuals has several distinct phenotypic features, and these patients should be classified as having multisystem progeroid syndrome (MSPS). MSPS patients should undergo careful assessment at symptom onset and yearly metabolic, renal, and cardiac evaluation because hyperglycemia, hypertriglyceridemia, FSGS, and cardiomyopathy cause major morbidity and mortality.

Keywords: lamin A/C, progeroid syndrome, focal segmental glomerulosclerosis, lipodystrophy, cardiomyopathy, diabetes mellitus

Heterozygous or biallelic pathogenic variants in the lamin A/C (*LMNA*) gene cause a spectrum of disorders, such as familial partial lipodystrophy of Dunnigan variety (FPLD2), muscular dystrophies, cardiomyopathies, neuropathy, and progeroid syndromes [1, 2]. The autosomal-dominant Hutchinson-Gilford progeria syndrome (HGPS) [3-5] and autosomal-recessive mandibuloacral dysplasia (MAD) are well-characterized distinct progeroid syndromes [6, 7], whereas atypical progeroid syndrome (APS) is more heterogeneous with variable clinical features [8]. About 90% of HGPS patients have a recurrent de novo heterozygous *LMNA* c.1824C>T; p.G608G pathogenic variant that activates a cryptic splice site resulting in production of the abnormal lamin A protein called progerin [3]. Patients with HGPS have a characteristic phenotype including narrow nasal tip, small mouth, thin lips, micrognathia, delayed eruption of primary and secondary teeth, loss of subcutaneous (sc) fat, alopecia, nail dystrophy, joint contractures, and hearing loss [4, 5]. HGPS patients die prematurely of myocardial infarction, heart failure, or cerebrovascular disease at a mean age of 13 years [4, 5]. APS is associated with a variety of heterozygous *LMNA* variants and presents with short stature, beaked nose, premature graying, and partial hair loss, high-pitched voice, skin atrophy over the hands and feet, partial or generalized lipodystrophy, skin pigmentation, and mandibular hypoplasia [8]. Recently, among approximately 40 reported patients with APS, we identified a distinct generalized lipodystrophy

associated progeroid syndrome (GLPS) affecting 11 patients due to a recurrent de novo heterozygous *LMNA* c.29C>T; p.T10I variant [9]. Similarly, 6 families with 11 affected patients have been reported to harbor a heterozygous *LMNA* c.1045C>T; p.R349W variant, with clinical features of partial lipodystrophy and interestingly show cardiomyopathy, and heavy proteinuria due to focal segmental glomerulosclerosis (FSGS) [10-15]. Here, we report 6 new patients with the heterozygous p.R349W *LMNA* variant from 4 families and review the previous literature to define unique characteristics of this progeroid syndrome.

1. Materials and Methods

We studied 4 probands and their relatives with the heterozygous *LMNA* p.R349W variant (Fig. 1). Multisystem progeroid syndrome patients (MSPS) 100.5 and MSPS 200.4 were evaluated at UT Southwestern Medical Center (UT Southwestern); records were obtained for patient, MSPS 200.1; patients MSPS 100.3 and MSPS 100.7 were evaluated in Darlinghurst, Australia; patient MSPS 300.3 at Vanderbilt University Medical Center and UT Southwestern, and patient MSPS 400.3 in Belo Horizonte, Brazil, and the University of Washington. The research protocol was approved by the respective institutional review boards, and all participants provided written informed consent.

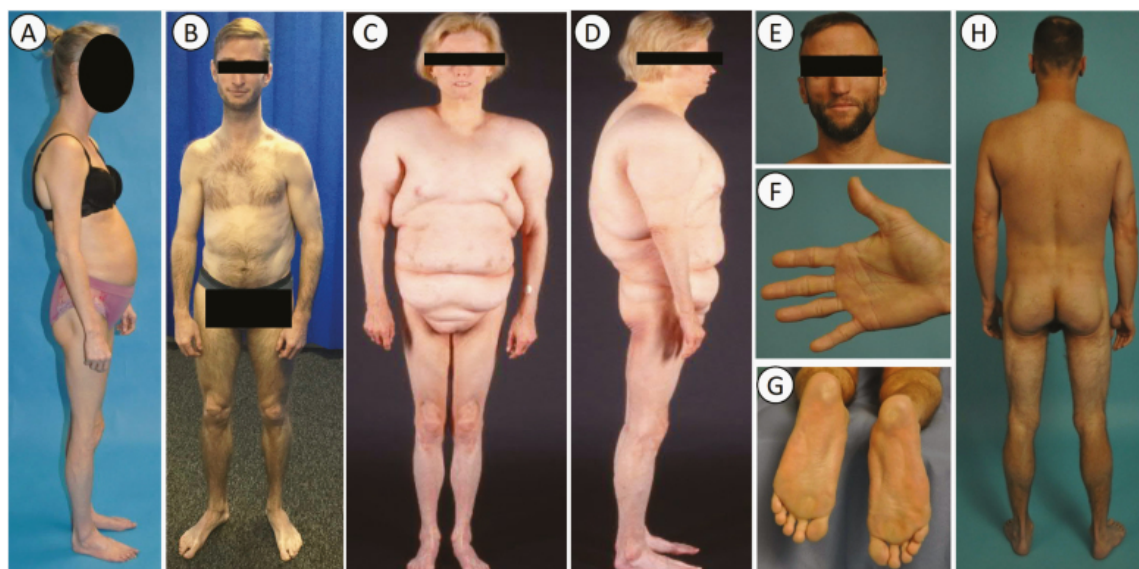


Figure 1.

Phenotypic features of patients with multisystem progeroid syndrome (MSPS) with a heterozygous lamin A/C (*LMNA*) p.R349W (c.1045C>T) variant. All patients have marked subcutaneous (sc) fat loss from the lower extremities, soles, and palms; and have more sc fat in the upper body, including the abdomen and shoulders. A, Lateral view of patient MSPS 100.5, a 42-year-old white woman with loss of sc fat from the legs and arms, and a protuberant abdomen. She had a thin face with sunken eyes and cheeks prior to getting fillers. B, Anterior view of patient MSPS 100.7, a 29-year-old man showing markedly muscular habitus due to loss of sc fat from the upper and lower extremities. C, Anterior and D, lateral views of patient MSPS 200.4, a 33-year-old white woman with fat loss from the lower extremities including the gluteal region, and excessive sc fat on the upper arms, shoulders, back, and abdomen, but not on the breasts. She had a birdlike face with sharp features and gray hair. E, Face, F, palm, G, soles, and H, posterior view of patient MSPS 300.3, a 30-year-old white man with sunken cheeks and fat loss from the palms and soles. He had marked loss of sc fat from the lower arms, legs, and gluteal region.

A. Anthropometry

Height, body weight, and skinfold thickness were measured by standard procedures as reported previously [8]. Whole-body and regional fat in the head, trunk, and upper and lower extremities were determined using Hologic QDR-4500A or Discovery W (S/N 84310). Whole-body magnetic resonance imaging (MRI) study was performed using a 1.5 Tesla imaging device (Philips Medical Systems) and version 5.2-2 software as reported previously [8]. The patient was evaluated using a 10-mm-thick T1 imaging technique with a repetition time of 580 ms, an echo time of 8 ms, and a 384×512 matrix combined with a 45-cm field of view.

B. Biochemical Analyses

Plasma glucose, serum cholesterol, triglycerides, high-density lipoprotein cholesterol, and chemistry as well as blood hemoglobin A_{1c} (HbA_{1c}) were analyzed as part of a systematic multichannel analysis. Serum leptin levels were measured by electrochemiluminescence assay (Quest Diagnostics) [16, 17] in patient 300.3 (normal range, 0.3-13.4 ng/mL, interassay coefficient of variation (CV) 4.1%-5.5% and intra-assay CV 4.7%-9.7%), and by radioimmunoassay in patients 100.7 and 400.3 (Linco Research, currently EMD Millipore [18]; interassay CV 6.5%-8.7% and intra-assay CV 2.8%-3.6%, normal range, 5.6-13.0 ng/mL). Urine protein excretion was measured by Quest Diagnostics using colorimetric spectrophotometry method (reference range, < 0.15 g/d) for patients 100.5, 200.4, and 300.3; by the benzethonium chloride method on a Roche Modular analyzer for patient 100.7 (Roche Diagnostics), and by the colorimetric method (pyrogallol red) for patient 400.3.

C. Genetic Variants Detection

C-1. **Genotyping** Patient MSPS 100.3 was genotyped for *LMNA* using Sanger sequencing at UT Southwestern. MSPS 100.5 and 100.7 were genotyped in the research setting University of Cambridge, Cambridge, UK. Patient MSPS 200.4 underwent exome sequencing using the Integrated DNA Technologies xGen Exome Research Panel v1.0 on the Illumina platform at UT Southwestern. MSPS 300.3 was sequenced using a targeted next-generation sequencing panel with linked bioinformatics [19] and was confirmed by Sanger sequencing. The family members of MSPS 200.4 and MSPS 300.3 were genotyped using Sanger sequencing at UT Southwestern. The exons and exon-intron boundaries of the *LMNA* gene were sequenced as reported previously [20].

Patient MSPS 400.3 underwent exome sequencing as described previously [21] and was confirmed with Sanger sequencing by the International Registry of Werner Syndrome.

D. RNA Extraction and Reverse Transcriptase–Polymerase Chain Reaction

Total RNA was prepared from fibroblasts from an unaffected and affected subject using RNA STAT-60 (Tel-Test Inc). A total of 20 µg RNA was DNaseI treated (30 minutes at 37°C) using the DNase-free kit from Ambion. Complementary DNA (cDNA) was synthesized from RNA at 25°C for 10 minutes; 48°C for 30 minutes followed by 95°C for 5 minutes using the reverse transcription kit from ABI. To determine the effect of *LMNA* c.1045C>T in inducing alternate splicing, cDNA was amplified with primers located in exons 5 and 7 (F1 5'-GGCAGTCTGCTGAGAGGAAC-3' plus R1 5'-ACAACTTGCCCTCCTCATC-3'). cDNA was amplified using a touchdown polymerase chain reaction protocol as follows: 98°C for 5 minutes followed by 20 cycles at 96°C for 30 seconds, 65°C for 30 seconds with a 0.5°C decrease each cycle, 72°C for 30 seconds and an additional 20 cycles at 96°C for 30 seconds, 55°C for 30 seconds, and 72°C for 30 seconds. The amplified products were analyzed on 1.2% agarose gel and visualized with ethidium bromide. The DNA fragment was of the expected 532-base pair size.

E. Western Blotting

Total protein extract was resolved on a 7.5% sodium dodecyl sulfate–polyacrylamide gel. Lamin A/C was probed with anti-Lamin A/C (E-1, mouse monoclonal antibody, 1:2500 dilution, (Santa Cruz Biotechnology, Inc) [22] for 2 hours at room temperature. Immunoblot was incubated with secondary antibody, mouse immunoglobulin (Ig)Gκ binding protein conjugated to horseradish peroxidase (1:2500 dilution, Santa Cruz Biotechnology, Inc) [23] for 1 hour at room temperature. Proteins were detected by exposure to x-ray film using chemiluminescent reagents. Blot was stripped and reprobed for GAPDH (glyceraldehyde-3-phosphate dehydrogenase) with anti-GAPDH at 1:50 000 dilution (Thermo Fisher) [24] for 1 hour at room temperature. Secondary antibody was the same as described previously.

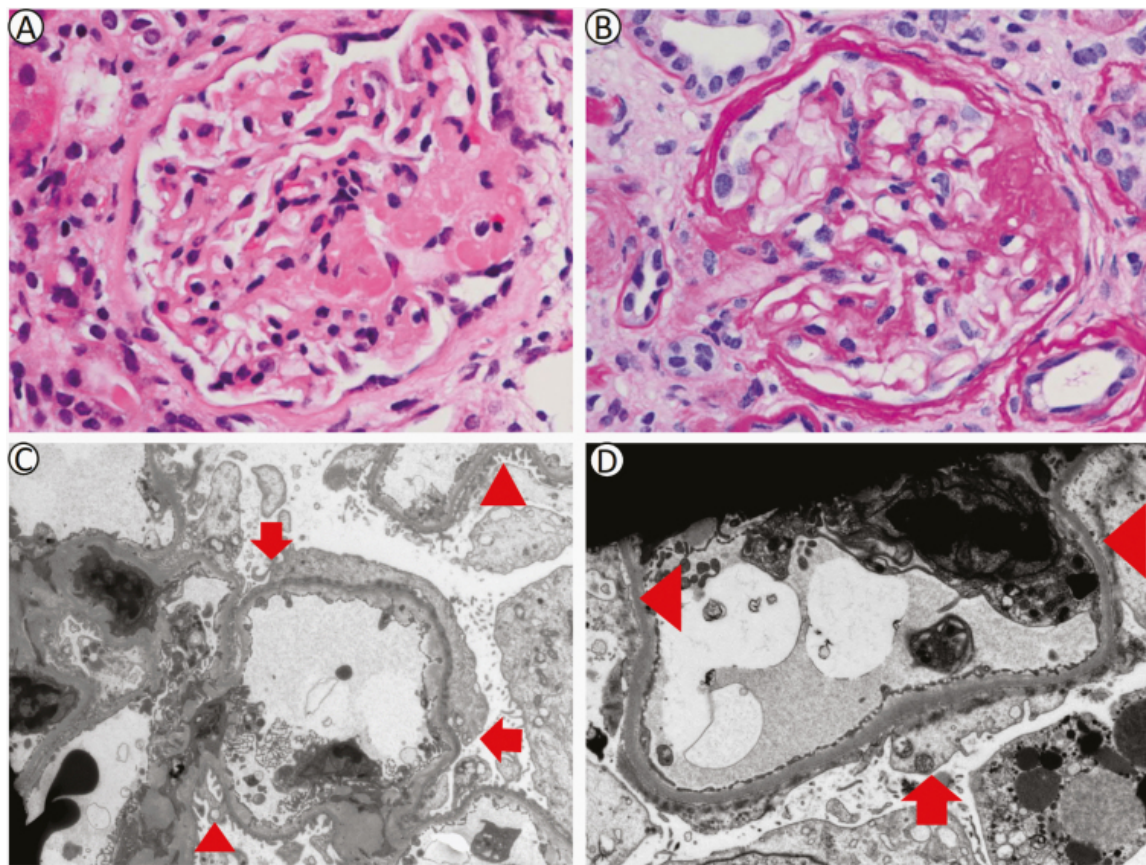
F. Immunofluorescence Microscopy

Human dermal fibroblasts were grown on cover slips in a 6-well plate a day before the experiment. The following day, the cells were fixed and permeabilized by incubating them with methanol (−20°C) for 20 minutes. Cells were washed 3 times for 5 minutes with phosphate-buffered saline (PBS) and then incubated with primary antibody against lamin A/C (E-1, or lamin B1 [L1220-20, mouse monoclonal antibody, US Biological; www.usbio.net]) [25] at a dilution of 1:100 for 60 minutes at 37°C in a humidified chamber. Cells were then washed 3 times for 5 minutes with PBS and incubated with AlexaFluor-568–coupled fluorescent secondary antibody (Invitrogen) [26] for 60 minutes at 37°C in a humidified chamber. After incubation, cells were washed 3 times for 5 minutes with PBS, counterstained with 4′-6-diamidino-2-phenylindole (DAPI) during the washes, and mounted on a glass slide with Aqua Poly/Mount (Polysciences). Cells were observed with DeltaVision RT Deconvolution Microscope (Applied Precision). Z-stack images for red and blue fluorescence were acquired in 0.15-μm steps at 60× magnification and were deconvolved using SoftWoRx (Applied Precision). Images were further processed using Imaris software (Bitplane).

G. Case Reports

G-1. Multisystem progeroid syndrome 100.5 This 44-year-old white woman presented with gradual loss of sc fat from the hips, legs, and breasts since age 20 years. By age 33, she had significant fat loss from the face, with sunken cheeks, pointed nose, and thin lips and later required fillers in the cheeks. She was 165 cm tall and weighed 46.4 kg. Physical examination revealed significant sc fat loss from the palms and soles, and thin extremities with a protruding abdomen ([Fig. 1A](#)). She did not have acanthosis nigricans and had excess fat on her trunk and back.

She developed diabetes mellitus at age 31 and was treated with metformin. She developed hypertension, hyperlipidemia (highest serum triglycerides over 500 mg/dL), and renal disease with proteinuria (> 4.5 g in 24 hours) at age 38. Renal biopsy showed FSGS, with 70% foot process effacement that was not immune mediated ([Fig. 2](#)).



[Open in a separate window](#)

Figure 2.

Histopathology of a kidney from patient MSPP 100.5. Renal biopsy shows segmental sclerosis lesions typical of focal segmental glomerulosclerosis at 600 \times magnification. A, Hematoxylin-eosin stain shows a glomerulus with a sclerotic segment at right containing an increased mesangial matrix, with closed capillary loops, adhesion to Bowman capsule, and hyaline insudates. B, Periodic acid–Schiff stain shows the vascular pole to the left, and a cap of segmental sclerosis with a synechia (adhesion) to the Bowman capsule at the right. C, Ultrastructural examination of 2 glomeruli show open capillary loops, with podocyte foot process effacement involving 50% to 60% of sampled capillary loop surfaces (center, original magnification about 6000 \times). Podocyte foot processes are fused between the 2 arrows. Podocyte foot processes are intact near the 2 triangles. Capillary loop basal lamina show some thin segments, without multiple layers of duplication, without mesangial matrix expansion in these 2 glomeruli, and without dense deposits in the subepithelial, subendothelial, or mesangial areas. D, Higher-power electron micrograph shows effacement of podocyte foot processes over most of this capillary loop, with minor thinning of the basal lamina (original magnification approximately 9600 \times). Podocyte foot processes are fused at the arrow, with a normal thick, gray band of basal lamina above. A thinner gray band of basal lamina appears to the left of the triangles.

At age 39, she was diagnosed with cardiomyopathy, with a left ventricular ejection fraction of 40% to 45%, and global hypokinesis. Her echocardiogram showed mild mitral regurgitation, mild tricuspid regurgitation, and trace aortic regurgitation. She had hospitalizations secondary to hypertensive urgency.

Her total fat by dual-energy x-ray absorptiometry (DEXA) was low (23.7%): in the 11th percentile for young normal and 5th percentile for age-matched controls. Her lower extremities had less fat (12.7%), with trunk (27.7%) and upper extremities (32.2%) showing more fat. Her bone density was normal. She had scoliosis of the lumbar spine. Abdominal ultrasound done at age 40 showed mild fatty liver, along with renal and pancreatic cysts. She had regular menstrual periods with heavy blood flow, but she never became pregnant.

She developed laryngeal cancer at age 44, requiring surgery and radiation therapy. Her mother was affected and also had proteinuria and sensorineural hearing loss and died at age 43 of cardiomyopathy. Her affected sister (MSPS 100.3) died at age 45 of pharyngeal/esophageal cancer. Her affected younger brother, age 40 at the time of evaluation, had cardiomyopathy with a defibrillator and a pacemaker, and also had end-stage renal disease secondary to FSGS, requiring dialysis. Her brother's daughter was reported to have a similar body shape with thin legs and protruding abdomen.

G-2. Multisystem progeroid syndrome 100.3 This 45-year-old, elder sister of MSPS 100.5, was diagnosed at age 39 years with diabetes, which was well controlled on glipizide with blood HbA_{1c} of 6.9%. She had no diabetic retinopathy or neuropathy but she had marked proteinuria with urinary albumin-to-creatinine ratio of 513 mg/mmol (normal range < 3.5 mg/mmol).

She had menarche at age 13 and had regular menstrual periods. She had one normal pregnancy resulting in birth of discordant twins. She first noted facial fat loss at age 21. She was diagnosed with hypothyroidism at age 41. She had long-standing sensorineural deafness. She had surgery for scoliosis at age 17.

Examination revealed a height of 150 cm, with a weight of 49.7 kg. She had prominent loss of sc fat from the face and buttocks. She had a small beaked nose and knobby knuckles. She had a scar from previous scoliosis surgery. She had a systolic ejection murmur. Echocardiography revealed mild mixed aortic valve disease with normal left ventricular size and systolic function.

Biochemical testing revealed hypertriglyceridemia (serum triglycerides 399 mg/dL). She was advised to take atorvastatin and fenofibrate for hypertriglyceridemia and metformin for diabetes control.

Despite being a never smoker, she was diagnosed with synchronous squamous cell carcinomas of the pharynx and esophagus at age 43. She underwent surgery and adjuvant chemoradiotherapy. She died of multiorgan failure at age 45 with complicating pneumonia.

G-3. Multisystem progeroid syndrome 100.7 This 29-year-old man, son of patient MSPS 100.3, first noticed body fat loss affecting his face at age 19 years, followed by his limbs ([Fig. 1B](#)). His twin sister was unaffected. He had normal pubertal development. He developed diabetes mellitus, hypertension, hyperlipidemia, and hepatic steatosis at age 18. These have been well managed with metformin, perindopril, and dietary modifications. He developed proteinuria at age 22, with recent 24-hour urinary protein excretion of 1.43 g/day, which was out of proportion to his well-controlled diabetes with blood HbA_{1c} of 5.1%. He had scoliosis with onset in his early teens and required fusion of 4 lumbar vertebrae at age 15, to reduce his scoliosis from 72° to 64°.

At age 25, he developed pericarditis. At age 27, he presented with exertional dyspnea and was found to have mild to moderate concentric left ventricular hypertrophy with an ejection fraction of 45% with diastolic dysfunction. He developed acalculous cholecystitis at age 29, when a significant deterioration in his cardiac function (ejection fraction 20%) and severe diastolic dysfunction were noted, and an implantable cardioverter defibrillator was placed, with an increase in ejection fraction to 37%.

On examination, his weight was 53.9 kg at first presentation and height was 166 cm. He had a scar from previous scoliosis surgery. He had a progeroid appearance with a beaked nose, a small chin, and striking fat loss involving his face, extremities, and buttocks, but sparing his abdomen. He had loss of

muscle bulk in his lower limbs.

G-4. Multisystem progeroid syndrome 200.4 This 33-year-old white woman developed sc fat loss from the lower extremities and forearms at age 10 years, and fat accumulation on the arms, shoulders, chest, and abdomen that gradually progressed ([Fig. 1C](#) and [1D](#)). She was diagnosed with hypertriglyceridemia at age 18 and was noted to have serum triglyceride concentrations over 1000 mg/dL on multiple occasions. She had menarche at age 12 and had regular menstrual periods until age 33 when she stopped taking oral contraceptive pills. Short stature (height, 148.6 cm) and shield chest prompted evaluation for Turner and Noonan syndromes, which were negative.

On physical examination her pulse was 84 beats/minute and blood pressure was 150/76 mm Hg, and her weight was 53 kg. She had bird facies, high-pitched voice, and mild sensorineural hearing loss since age 6 to 8. She had micrognathia with dental overcrowding requiring extensive dental work and a chin implant at age 18 (removed after infection), and chronic sinusitis that improved after rhinoplasty at age 15 and sinus surgery at age 22. She had pronounced fat loss from the palms and soles (requiring foot arthrodesis for walking), buttocks, lower extremities, and the genital area. She had excessive fat on the arms, shoulders, chest, and abdomen (see [Fig. 1C](#) and [1D](#)).

Whole-body DEXA scan revealed total body fat of 37%, with upper extremity fat of 58.4%, lower extremity fat of 16.2%, and truncal fat 40.7%. Her bone density was low for her age, and serum 25-OH vitamin D level was 12 ng/mL (reference range, 10-55 ng/mL; values < 30 ng/mL indicate vitamin D deficiency). She had loss of normal lordosis, and mild dextrorotatory scoliosis. There was mild hyperpigmentation over her trunk. She had a history of rheumatoid arthritis (rheumatoid factor: 37.8, reference: < 35) previously treated with methotrexate.

Whole-body MRI also showed a marked loss of sc fat from the lower extremities, especially from the calves and soles ([Fig. 3](#)). There was loss of sc fat from the lateral and anterior-posterior thigh regions with some preservation of sc fat in the medial thighs. There was also reduced sc fat in the forearms, but sc fat was increased in the proximal region of upper arm near the shoulders. She also had increased sc fat in the upper trunk. The mediastinum, omentum, and retroperitoneal regions had somewhat reduced amounts of fat.

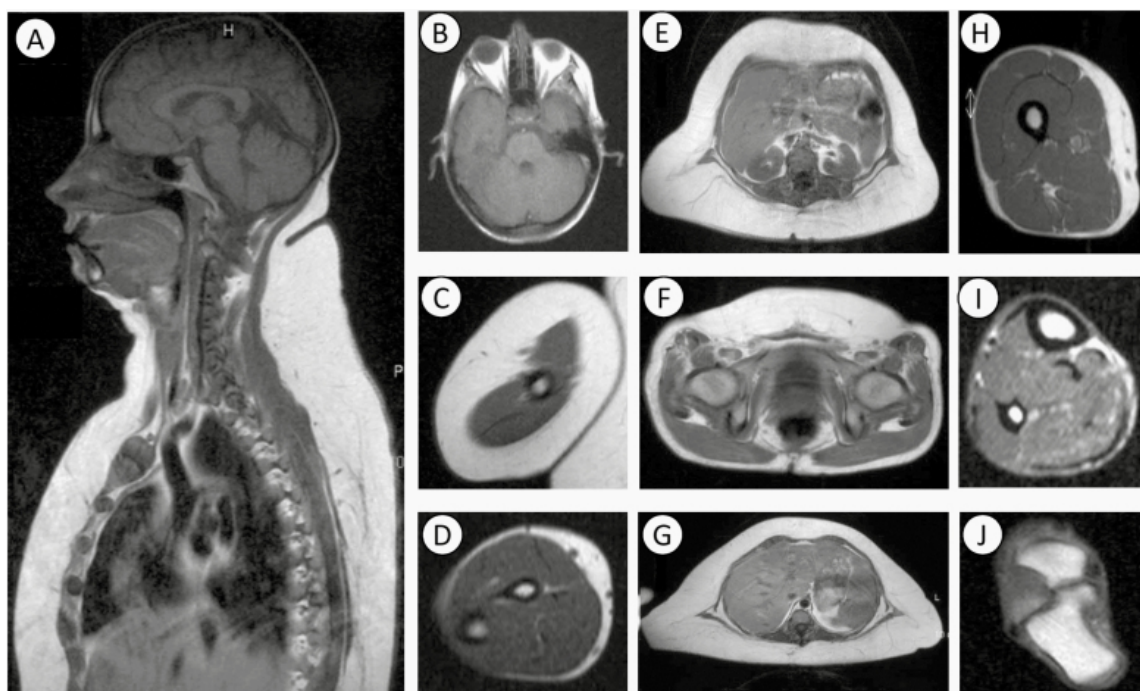


Figure 3.

T1-weighted MRIs of patient MSPS 200.4 for body fat distribution. A, Sagittal MRI through the head and thorax at midline shows reduced subcutaneous (sc) fat on the head but increased sc fat in the neck and thorax anteriorly and posteriorly. Axial MRI, B, through the head at the level of the eyes shows normal orbital and sc fat in the temporal and occipital regions; C, through the upper arm shows excess sc fat; D, through the forearm shows marked loss of sc fat from the anterior, lateral, and posterior regions; E, through the abdomen at the level of the kidneys shows reduced perirenal fat but marked excess of sc fat around abdomen; F, through the pelvis at the level of the hip joint shows markedly reduced sc fat posteriorly but increased sc fat anteriorly; G, through the upper abdomen at the level of the liver shows increased sc fat; H, through the thigh shows reduced sc fat from the anterior, lateral, and posterior regions but preservation of sc fat medially; I, through the calf shows markedly reduced sc fat; and J, through the foot shows lack of sc fat in the plantar region.

Other comorbidities included hypertension, and chronic kidney disease since age 31. A 3-day sample of urine was collected that showed an average urine protein excretion of 442 mg/day, and a protein/creatinine ratio of 489 mg/g at the time of initial evaluation. Her kidney disease progressed, and she later had total protein excretion of 2.47 g/day.

She had frequent hospital admissions for cardiomyopathy (congestive heart failure and atrial fibrillation). Echocardiogram at age 33 showed a left ventricular ejection fraction of 50%, and moderate aortic stenosis. Subsequent echocardiogram a few months later showed an ejection fraction of 10%, moderate pulmonary hypertension, and pleural effusion. She also developed conduction abnormalities. She died of bacterial endocarditis at age 36.

At autopsy, excess sc fat was noted on the upper arms, chest, and shoulders, and there was significant fat loss from the lower extremities and forearms. Measurements of sc fat were as follows: clavicle 35 mm, midabdomen 25 mm, midthigh 15 mm, and midcalf 0 mm. She was also noted to have thin mesentery. The heart weighed 340 grams. Pathology showed moderate calcific coronary

atherosclerosis, involving right, circumflex, and anterior descending arteries, and patchy subendocardial fibrosis, along with mild atherosclerosis of the aorta. She also had evidence of pulmonary congestion, mild pulmonary edema, and advanced arterial and arteriolar nephrosclerosis with atrophic kidneys (~ 75 g each). Ovaries were atrophic, with no ova or follicles. She had hepatomegaly with centrilobular passive congestion and atrophy and congestive splenomegaly.

G-5. Multisystem progeroid syndrome 200.1 This 34-year-old white man, the father of patient MSPS 200.4, reportedly died of a myocardial infarction. His height was 160 cm, and his body habitus was similar to his daughter, with fat loss from the lower extremities and accumulation of fat on the upper arms and torso. He had hyperlipidemia, and premature graying of the hair. His autopsy showed severe coronary arteriosclerosis with focal severe narrowing of both left and right coronary arteries, along with patchy myocardial fibrosis involving the anteroseptal myocardium, and a recent thrombus in right coronary artery, although no distinct area of acute myocardial infarction was seen. The heart weighed 360 grams, and the atria and ventricles were normal in size. Bilateral pleural effusions, right greater than left, were also noted. The kidneys weighed 220 grams each and had no significant lesions on microscopy.

G-6. Multisystem progeroid syndrome 300.3 This 30-year-old white man was diagnosed with lipodystrophy at age 29 years. He gradually lost fat from his face, arms, legs, and gluteal region in his 20s. Physical examination revealed fat loss from the palms and soles, face, and extremities but he did have some sc fat on his abdomen ([Fig. 1E-1H](#)). His liver was palpable 8 cm below the right costal margin. He had no joint contractures or deformities.

He had a congenital double aortic arch as an infant, with chronic pulmonary compromise, and underwent surgery at age 20 months. He was diagnosed with rheumatoid arthritis at age 12 years, and treated with methotrexate and adalimumab for a few months, but since then has remained off medications.

He was diagnosed with diabetes mellitus at age 17, with severe insulin resistance, requiring more than 450 units of insulin per day and complicated by nephrotic syndrome (> 4.9 grams of protein in 12 hours). His blood HbA_{1c} was 8.1%. He had a voracious appetite. He had severe hypertriglyceridemia (serum triglycerides > 5000 mg/dL), with eruptive xanthomas on the knees and elbows from age 25 to 27. Despite being on fenofibrate, fish oil, and atorvastatin, he has had 6 episodes of acute pancreatitis with the first at age 18, and 2 episodes when he was age 30. Acute pancreatitis at age 30 was associated with euglycemic diabetic ketoacidosis (in the setting of empagliflozin use) and non-ST elevation myocardial infarction for which he underwent percutaneous intervention, and had a drug-eluting stent placed in the left anterior descending artery.

Echocardiogram showed normal left ventricular size with preserved left ventricular systolic function, with paradoxical septal motion and inferolateral hypokinesis. A nuclear stress test showed an estimated ejection fraction of 37% with a fixed inferolateral defect consistent with a prior infarct and no areas of reversible ischemia.

Whole-body DEXA scan showed a total body fat of 12.7% (sixth percentile compared to age-matched controls, and ninth percentile compared to young normal controls). There was more pronounced fat loss in the lower extremities (6.6%), followed by the trunk (14.4%) and the upper extremities (15.2%). His bone density was low for his age with a z score of -2.1. No scoliosis was observed. Computed tomography of the abdomen showed hepatic steatosis, and electrocardiogram revealed left axis deviation.

His father had high cholesterol, hypertension, and tachycardia but no lipodystrophy. His mother, brother, and a 7-month-old child are all healthy.

G-7. Multisystem progeroid syndrome 400.3 This 36-year-old white woman was noted to have thin legs at age 7 years. She noted pronounced fat loss at age 18 that involved her face and extremities but spared her trunk. She has had aesthetic procedures on her face and breast implants at age 18. On physical examination, her blood pressure was 120/80 mm Hg, heart rate was 68 beats/minute, and weight was 45.5 kg (body mass index: 17.5 kg/m²). Her hair was thin and sparse, and she had no acanthosis nigricans or hirsutism.

She had low bone density for her age (prior DEXA showed a z score of -0.5 in the spine and -2.1 in right femoral neck) and had previously been on alendronate for 3 years. She had no history of fractures. Workup for secondary causes showed hypercalciuria, which was treated with a thiazide diuretic.

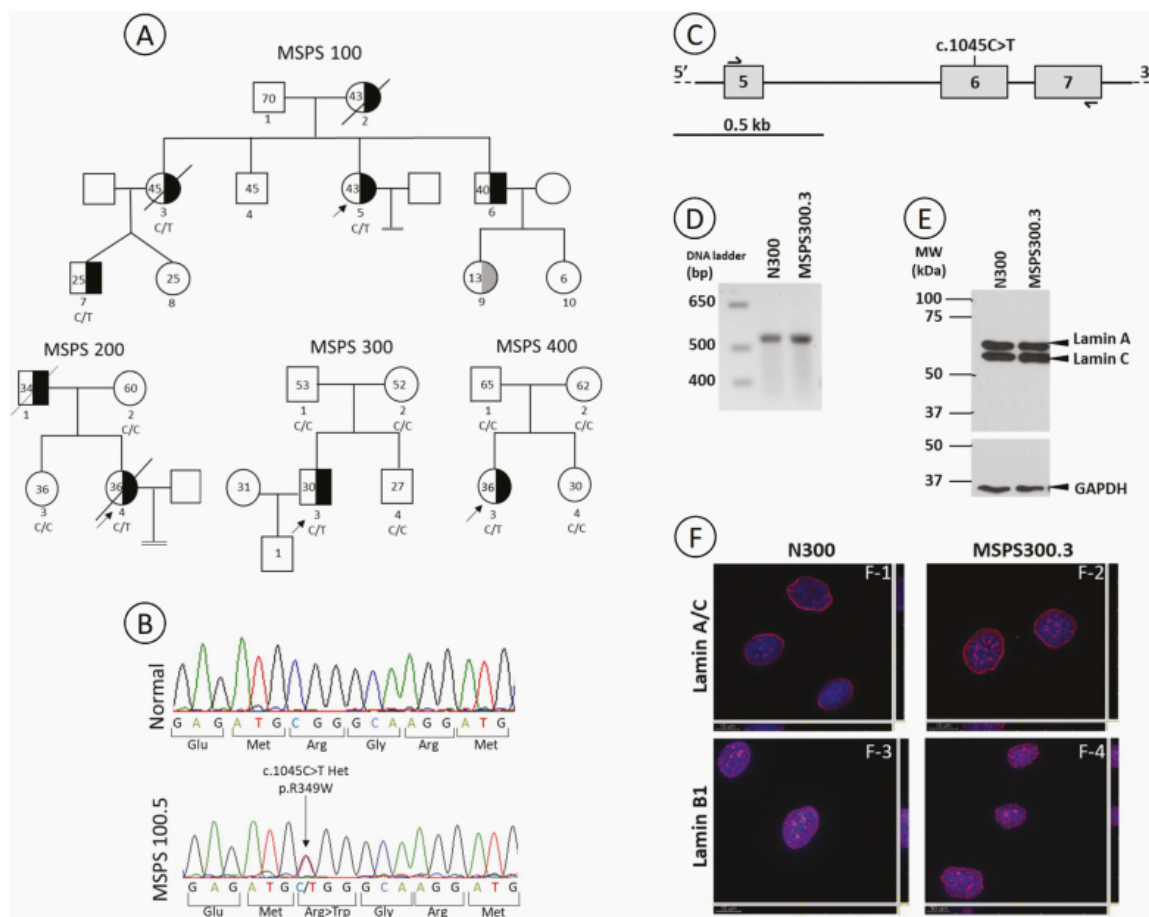
She was diagnosed with proteinuria (24-hour urine protein excretion of 491 mg) and hypertension at age 24. Renal ultrasonography showed increased bilateral cortical echogenicity. She was treated with losartan 50 mg daily and hydrochlorothiazide 12.5 mg daily. Her electrocardiogram showed left bundle branch block and transthoracic echocardiogram showed mild aortic, mitral and tricuspid regurgitation, and slight left ventricular hypertrophy with a preserved left ventricular ejection fraction of 72%.

At age 25, she developed diabetes mellitus and was treated with metformin 1000 mg daily and pioglitazone 30 mg daily. Her abdominal ultrasound showed moderate to severe hepatic steatosis. She developed mild hypertriglyceridemia after initiation of thiazide diuretic that did not require pharmacologic therapy.

She had irregular menstrual cycles in adolescence, which became regular in adulthood. Pelvic ultrasound showed ovaries with borderline volume suggesting chronic anovulation. She had normal genitalia and no hirsutism.

2. Results

All 6 patients from 4 unrelated families harbored a pathogenic heterozygous *LMNA* c.1045C>T; p.R349W variant (Fig. 4A and 4B). The phenotypic data for a total of 17 patients (12 female and 5 male), including 6 new patients and 11 previously reported patients, were reviewed, of whom 3 were children age 14 to 17 years (Table 1). Progeroid features such as premature graying, alopecia, and high-pitched voice were noted in several patients (see Table 1). Hearing loss (6 out of 9 patients), micrognathia (6 out of 9 patients) and scoliosis (6 out of 8 patients) featured prominently. All patients were reported to have lipodystrophy except for a 14-year-old girl, who may have been too young at the time of reporting to manifest clinical features. All adult patients had fat loss from both the extremities, although fat loss from the lower extremities was more pronounced than from the upper extremities, and distal regions (calves and forearms) were affected more than the proximal regions (thighs and upper arms). Skinfold thickness measurements in 2 female and 2 male patients also further confirm that the lower extremities are more affected with lipodystrophy than the upper extremities and that the fat loss is worse in the distal regions of the extremities (Fig. 5). Furthermore, lipodystrophy affected the face (11 out of 12 patients) and the palms and soles (10 out of 12 patients). A dorsal cervical fat pad was also noted in 5 out of 8 patients.



[Open in a separate window](#)

Figure 4.

Pedigrees of patients with multisystem progeroid syndrome (MSPS): Sanger sequencing showing the lamin A/C (*LMNA*) variant, partial gene structure of *LMNA*, alternative splicing, immunoblot for lamin A/C, and nuclear morphology of skin fibroblasts. A, The proband in each family is marked by a slanted arrow. Squares and circles represent males and females, respectively. Half-filled symbols indicate affected family members. The numbers inside the symbols indicate ages. C/C indicates wild-type *LMNA* nucleotides at c.1045, and C/T indicates the heterozygous c.1045C>T variant. In the MSPS 300 and 400 pedigrees, analysis of probands' parents revealed normal *LMNA* sequence suggesting de novo variants in the probands (MSPS 300.3 and 400.3). B, Chromatogram from Sanger sequencing *LMNA* exon 6 from normal and patient MSPS 100.5, showing the heterozygous c.1045C>T; p.R349W (arginine substituted by tryptophan) variant. C, Partial gene structure of *LMNA* drawn to scale. Exons 5 to 7 are shown as boxes and C > T nucleotide alteration is noted in exon 6. Location of primers used for amplification are marked as arrows. D, Amplified polymerase chain reaction (PCR) product from reverse-transcribed RNA was resolved on 1.2% agarose gel and visualized with ethidium bromide. Only one PCR product of expected size was observed from N300 (unaffected) and MSPS 300.3 (affected) individuals. E, Immunoblot for lamin A/C in N300 (unaffected) and MSPS 300.3 (affected) individuals. Lamins A and C are indicated by arrowheads. The antilamin A/C antibody raised against the epitope mapping to amino acids 2 to 29 in the amino terminus of the human protein will detect lamin at its the amino terminus. The immunoblot was stripped and reprobred with the antibody for GAPDH (glyceraldehyde-3-phosphate dehydrogenase). No abnormal protein band was seen in the affected individual. F, Nuclear morphology of dermal fibroblasts from N300 (unaffected) and MSPS 300.3 (affected) individuals. Shown are the representative z-stack images. Approximately 20 nuclei for each individual were observed. Lamin A/C (F1, F2) and lamin B1

(F3, F4) localize to the nuclear lamina. Localization in MSPS 300.3 (F2, F4) appears unaltered when compared to N300 (F1, F3). Red false coloring represents either lamin A/C or lamin B1, and blue false coloring represents DAPI (4',6-diamidino-2-phenylindole, dihydrochloride). All images were obtained under similar microscopic settings. Scale bar is 10 μm and is shown with the images.

Table 1.

Clinical features of patients with heterozygous *LMNA* p.R349W variant

	Prevalence	Our patients						Mory et al [11]	Akinci et al [12]		
Patient No.		100.3	100.5	100.7	200.4	300.3	400.3	14	9.1	9.2	9.3
Age at report, y		45	44	29	33	30	36	18	42	16	14
Age at onset of lipodystrophy, y		21	20	19	10	20s	18	12	20	15	NA
Sex	12 F/5 M	F	F	M	F	M	F	M	F	M	F
Short stature	4/9	Y	N	Y	Y	N	N	Y	NA	NA	NA
Diabetes mellitus	9/12	Y	Y	Y	N	Y	Y	N	Y	N	NA
Acanthosis nigricans	1/8	N	N	N	N	N	N	N	NA	NA	NA
Hypertriglyceridemia	12/13	Y	Y	Y	Y	Y	Y	Y	Y	N	NA
Hypertension	9/11	Y	Y	Y	Y	N	Y	N	NA	NA	NA
Coronary disease	4/9	N	N	N	Y	Y	N	NA	Y	N	NA
Cardiomyopathy	10/15	N	Y	Y	Y	Y	N	N	NA	N	NA
Micrognathia	6/9	Y	N	Y	Y	N	N	Y	Y	NA	NA
Fat loss: legs	16/17	Y	Y	Y	Y	Y	Y	Y	Y	Y	N
Fat loss: palms, soles	8/10	Y	Y	Y	Y	Y	N	Y	Y	NA	N
Fat loss: face	11/12	Y	Y	Y	Y	Y	Y	NA	Y	Y	N
Dorsocervical fat pad	5/8	N	Y	N	Y	Y	N	NA	NA	NA	NA
Hearing loss	6/9	Y	Y	N	Y	N	N	NA	Y	NA	NA
High-pitched voice	4/7	Y	Y	Y	Y	N	N	N	NA	NA	NA
Gray hair	4/8	Y	Y	N	N	Y	N	N	Y	NA	NA
Loss of hair	5/9	Y	N	N	N	Y	Y	N	Y	NA	NA
Hepatomegaly	9/10	N	Y	Y	Y	Y	Y	NA	Y	Y	NA
Proteinuria	13/14	Y	Y	Y	Y	Y	Y	NA	Y	N	NA
FSGS	7/7	NA	Y	NA	NA	NA	NA	NA	NA	NA	NA
Myopathy	4/9	N	N	N	NA	N	N	NA	Y	NA	NA
Scoliosis	6/8	Y	Y	Y	Y	N	N	NA	Y	NA	NA

[Open in a separate window](#)

Abbreviations: F, female; FSGS, focal segmental glomerulosclerosis; M, male; N, no; NA, not available; Y, yes.

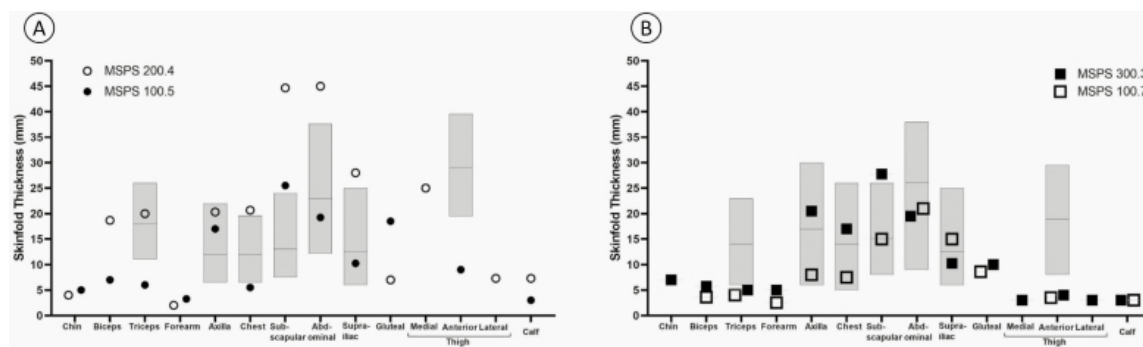


Figure 5.

Skinfold thicknesses of patients with multisystem progeroid syndrome (MSPS) with the heterogeneous lamin A/C (*LMNA*) p.R349W (c.1045C>T) variant. A, Skinfold thickness of 2 female patients, MSPS 200.4 (age 33 years) and MSPS 100.5 (age 44 years), marked by unfilled and filled circles, respectively. The gray bars show the 10th to 90th percentile values of normal age-matched women with the median value marked by a horizontal line [27]. B, Skinfold thickness of 2 male patients, MSPS 300.3 (age 30 years) and MSPS 100.7 (age 29 years) marked by filled and unfilled squares, respectively. The gray bars show 10th to 90th percentile values of normal age-matched men with the median value marked by a horizontal line [28]. All patients have markedly decreased skinfold thickness in the lower extremities and forearms, indicating partial loss of subcutaneous fat with normal or higher skinfold thickness in the abdominal region.

All adult patients for whom data were available had proteinuric nephropathy, and FSGS was documented in 7 of them. Two women, ages 33 and 37, had renal biopsies consistent with nephrosclerosis and thin basement membrane disease, respectively.

Cardiovascular complications were common, with 10 out of 15 patients developing cardiomyopathy, with coronary artery disease (4 patients), valvular disease (4 patients), and atrial fibrillation and other arrhythmias (7 patients) also being reported. Nine out of 11 patients were hypertensive. Two patients, both women, died early at ages 33 and 45, respectively. Presence of myopathy and low bone density was noted in 4 out of 8, and 5 out of 6 patients, respectively.

Metabolic complications, including diabetes mellitus (9 out of 12 patients), hypertriglyceridemia (12 out of 13 patients), and hepatomegaly (9 out of 10 patients), were highly prevalent (Tables 1 and 2). Interestingly, only one patient was reported to have acanthosis nigricans.

Table 2.

Metabolic parameters of patients with a heterozygous lamin A/C (*LMNA*) p.R349W variant

	Our patients						Mory et al [11]	Fountas et al [14]	van Tintelen et al [13]	Thong et al [10]	Ajluni et al [15]
Patient No.	100.3	100.5	100.7	200.4	300.3	400.3	14			1	22
Triglycerides, mg/dL	434	394	256	364	417	238	210	146	3623	NA	261
Cholesterol, mg/dL	204	207	166	226	186	208	150	226	NA	NA	NA
HDL-C, mg/dL	42.5	42	23	35.9	25	41	17	46	NA	NA	NA
HbA _{1c} , %	6.2	6.5	5.1	5.7	8.1	5.4	5.9	5.5	NA	NA	6.2
Glucose, mg/dL	144	125	112	75	164	109	NA	79	NA	NA	NA
Leptin, ng/mL	NA	NA	2.2	NA	3.1	6.6	2.2	26.1	31.1	NA	55.4
Proteinuria, g/d	NA	7	1.52	2.47	9.85	0.39	NA	2.2	NA	2.7	NA
Lipid-lowering drugs	Y ^a	Y ^b	N	Y ^c	Y ^d	N	NA	NA	NA	NA	N

[Open in a separate window](#)

Abbreviations: HbA_{1c}, hemoglobin A_{1c}; HDL-C, high-density lipoprotein cholesterol; N, no; NA, not available; Y, yes.

^aAtorvastatin 40 mg and fenofibrate 145 mg daily.

^bAtorvastatin 20 mg daily.

^cGemfibrozil 600 mg twice daily.

^dAtorvastatin 40 mg, fenofibrate 145 mg, and fish oil 4 g daily.

The heterozygous c.1045C>T variant in exon 6 of *LMNA* will result in a conserved dinucleotide splice donor site, “GT,” which may well generate an altered *LMNA* transcript. To determine this, we amplified the cDNA generated from normal and MSPS 300.3 fibroblasts with primer pairs located in exons 5 and 7 (Fig. 4C). The amplified polymerase chain reaction product resolved in an agarose gel were of similar size both in the normal control and affected individual (Fig. 4D). This suggested that despite the generation of a possible splice donor, “GT,” an altered *LMNA* transcript was not observed. Sanger sequencing of the amplified product further confirmed this observation. Immunoblot analysis of the protein lysates of the fibroblasts showed no additional abnormal protein bands (Fig. 4E).

To investigate whether the heterozygous c.1045C>T *LMNA* variant results in any nuclear blebbing or dysmorphology, we performed indirect immunofluorescence localization of lamin A/C and lamin B1 in skin fibroblasts. Lamin A/C protein localized to the nuclear inner membrane as expected and no nuclear blebbing/dysmorphology was observed (Fig. 4F). Likewise, indirect immunofluorescence localization of lamin B1, another nuclear lamina protein, did not reveal any abnormal nuclear morphology in skin fibroblasts of the affected patient (Fig. 4F).

3. Discussion

Our report of 6 new patients with the pathogenic heterozygous *LMNA* p.R349W variant and the review of previously published patients in the literature with the same variant [10-15] highlights several characteristic phenotypic features that are distinctive from those caused by other variants in the same gene. These include progeroid features, a peculiar pattern of partial lipodystrophy, cardiomyopathy, and proteinuric nephropathy.

Many patients had progeroid features and they looked much older than their age not only because of loss of sc fat from the face, but also because of premature graying of the hair and alopecia. In addition, they had micrognathia, high-pitched voice, and hearing loss. All affected adults had a peculiar pattern of lipodystrophy, with fat loss from the face and both extremities, with the legs affected more than the arms and more fat loss from the distal regions (forearm and calf) than from the proximal regions (upper arms and thighs). In addition, all affected adults had fat loss from the palms and soles. Using MRI, Akinçi et al [12] demonstrated a distinctive fat loss pattern in their patient with the heterozygous *LMNA* p.R349W variant with lipodystrophy of the face and limbs (more pronounced in distal parts), as opposed to the pattern associated with other variants in the *LMNA* gene. Whole-body MRI in one of our patients further confirms the unique pattern of lipodystrophy in patients with the *LMNA* heterozygous p.R349W variant. This pattern is very different from that seen in patients with familial partial lipodystrophy, Dunnigan variety [29], as well as in those with mandibuloacral dysplasia type A [30], who lose sc fat from the extremities and trunk but gain sc fat in the face and do not lose fat from the palms and soles. It is also different from that seen in patients with GLPS with the *LMNA* heterozygous p.T10I variant who have near generalized loss of sc fat from the face, extremities, trunk, and palms and soles without accumulation of sc fat in the truncal region [9]. HGPS patients also have near generalized loss of sc fat, but they develop only minimal metabolic complications [3, 4]. APS patients do present with variable patterns of lipodystrophy and some develop cardiomyopathy, but proteinuria is not prevalent among them [8].

Another unique feature of this syndrome is proteinuria. Whereas some patients have been reported to have FSGS on kidney biopsy, others had a different pathology, including nephrosclerosis and thin basement membrane disease. Nearly all our patients had gross proteinuria, and some had markedly increased proteinuria in the nephrotic range. Interestingly, we previously reported FSGS in patients with type B mandibuloacral dysplasia due to biallelic *ZMPSTE24* variants [31]. However, other patients with HGPS, GLPS, and APS have not been reported to have FSGS [4, 5, 8].

The third unique feature of these patients is cardiomyopathy. Based on 2 autopsy reports in our patient and her father, subendocardial fibrosis and coronary atherosclerosis may both be involved in causing cardiomyopathy and need for cardiac transplantation. In addition, valvular disease and arrhythmias may further compromise cardiac function.

Metabolic complications are also highly prevalent in these patients, with diabetes, hypertriglyceridemia, and hepatomegaly/hepatic steatosis affecting more than 75% of the adult patients. In addition, impaired glucose tolerance, hyperinsulinemia, as well as polycystic ovary disease

[14, 15] have been reported. The onset of metabolic complications can be as early as age 12 years [11]. Interestingly, acanthosis nigricans, which is common in FPLD2 patients, was reported in only 1 out of 8 patients with the heterozygous p.R349W variant [14].

Among other manifestations, 6 patients had scoliosis and 2 of our patients required corrective surgery. However, as compared to patients with HGPS and MAD, our patients did not have acro-osteolysis, mandibular hypoplasia, or clavicular hypoplasia [3-5, 30]. Two patients were possibly misdiagnosed with rheumatoid arthritis, as joint pain and contractures could be part of the syndrome. Two female patients belonging to the MSPS 100 pedigree developed pharyngeal/laryngeal carcinoma; however, whether it is associated with the heterozygous *LMNA* p.R349W variant remains uncertain.

We also investigated why the heterozygous *LMNA* p.R349W variant causes distinctive clinical manifestations. Although in silico splice-site prediction programs such as SPANR [32] and ASSP [33] gave inconsistent predictions on whether the c.1045C>T variant may induce an alternate splice site, cDNA sequencing from skin fibroblasts did not detect alternative splicing. Furthermore, we did not observe any unusual protein product on immunoblot. Lastly, the morphology of the nuclei from skin fibroblasts of one of the patients did not reveal any striking abnormalities as have been reported by us previously in some patients with APS [8], and by others in HGPS [34, 35] or mandibuloacral dysplasia [36, 37] due to various *LMNA* variants. Thus, it is unclear why the heterozygous *LMNA* p.R349W variant results in multisystem pathology. It is still possible that this variant causes tissue-specific alternate splicing, for example, in the kidneys and heart, which can be confirmed only if such tissues are available from the affected patients.

Variants in the *LMNA* gene result in a variety of clinical disorders but the underlying mechanisms of allelic and clinical heterogeneity remain unclear. Interestingly, *LMNA* has been associated with the largest and most diverse number of disease-linked variants in the human genome, with 683 *LMNA* variants reported in Clinvar (<https://www.ncbi.nlm.nih.gov/clinvar/>), out of which 171 are reported as pathogenic [38]. Among the various mechanisms suggested for allelic heterogeneity include changes in heterochromatin formation at the nuclear envelope (epigenomics), perturbing gene-silencing programs during terminal differentiation of cells, modulation of interactions between lamins and the histone H2A/H2B dimer due to altered phosphorylation, and structural abnormalities of the nuclear membrane [38]. Other investigators [39] also suggested loss of interaction between lamin A/C and various splicing factors may be responsible for tissue specific effects of lamin A/C variants.

In conclusion, patients with the heterozygous *LMNA* p.R349W variant have distinct clinical features and severe metabolic complications. We propose that they be recognized as having MSPS. MSPS patients should undergo careful multisystem assessment at onset and yearly general, metabolic, renal, and cardiac evaluation because hyperglycemia, hypertriglyceridemia, proteinuric nephropathy, and cardiomyopathy are the major contributors to morbidity and mortality.

Acknowledgments

We thank Carmel Tovar for illustrations, Katie Tunison for assistance with immunoblotting and RNA sequencing experiments, Claudia Quittner for help with evaluation of patients, Nivedita Patni, MD, for performing the skin biopsy of patient 300.3 at the UT Southwestern Medical Center, Addenbrooke Molecular Genetics Lab for genotyping *LMNA* variant in 2 of the patients, and the patients and their families for participating in this study.

Financial Support: This work was supported by the National Institutes of Health, (Grant R01-DK105448), Clinical and Translational Science Awards (Grants UL1RR024982, UL1TR001105, UL1TR000433, and R01-CA210916), and the Southwestern Medical Foundation.

Author Contributions: I.H. and A.G. designed the study, reviewed the data and literature, collected and interpreted the data, and wrote the first draft. R.R.J and K.H.C.W co-contributed to part of the initial draft. H.B., J.R.G., S.D., C.X., R.A.H., B.G.C-L., M.F.L., F.V., K.H.C.W., D.R.P., J.O., and A.K.A. provided additional data, interpretation, and reviewed, commented, and edited the manuscript.

Glossary

Abbreviations

APS	atypical progeroid syndrome
cDNA	complementary DNA
DEXA	dual-energy x-ray absorptiometry
FPLD	familial partial lipodystrophy
FSGS	focal segmental glomerulosclerosis
GLPS	generalized lipodystrophy associated progeroid syndrome
HGPS	Hutchinson-Gilford progeria syndrome
LMNA	lamin A/C
MAD	mandibuloacral dysplasia
PBS	phosphate-buffered saline
sc	subcutaneous

Additional Information

Disclosure Summary: The authors have no conflicts of interest to disclose.

Data Availability: All data generated or analyzed during this study are included in this published article or in the data repositories listed in “References and Notes.”

References and Notes

1. Jacob KN, Garg A. Laminopathies: multisystem dystrophy syndromes. *Mol Genet Metab.* 2006;87(4):289-302. [[PubMed](#)] [[Google Scholar](#)]
2. Broers JL, Ramaekers FC, Bonne G, Yaou RB, Hutchison CJ. Nuclear lamins: laminopathies and their role in premature ageing. *Physiol Rev.* 2006;86(3):967-1008. [[PubMed](#)] [[Google Scholar](#)]
3. Eriksson M, Brown WT, Gordon LB, et al. . Recurrent de novo point mutations in lamin A cause Hutchinson-Gilford progeria syndrome. *Nature.* 2003;423(6937):293-298. [[PubMed](#)] [[Google Scholar](#)]
4. Merideth MA, Gordon LB, Clauss S, et al. . Phenotype and course of Hutchinson-Gilford progeria syndrome. *N Engl J Med.* 2008;358(6):592-604. [[PMC free article](#)] [[PubMed](#)] [[Google Scholar](#)]
5. Hennekam RC. Hutchinson-Gilford progeria syndrome: review of the phenotype. *Am J Med Genet A.* 2006;140(23):2603-2624. [[PubMed](#)] [[Google Scholar](#)]

6. Simha V, Agarwal AK, Oral EA, Fryns JP, Garg A. Genetic and phenotypic heterogeneity in patients with mandibuloacral dysplasia-associated lipodystrophy. *J Clin Endocrinol Metab.* 2003;88(6):2821-2824. [[PubMed](#)] [[Google Scholar](#)]
7. Novelli G, Muchir A, Sanguolo F, et al. . Mandibuloacral dysplasia is caused by a mutation in *LMNA*-encoding lamin A/C. *Am J Hum Genet.* 2002;71(2):426-431. [[PMC free article](#)] [[PubMed](#)] [[Google Scholar](#)]
8. Garg A, Subramanyam L, Agarwal AK, et al. . Atypical progeroid syndrome due to heterozygous missense *LMNA* mutations. *J Clin Endocrinol Metab.* 2009;94(12):4971-4983. [[PMC free article](#)] [[PubMed](#)] [[Google Scholar](#)]
9. Hussain I, Patni N, Ueda M, et al. . A novel generalized lipodystrophy-associated progeroid syndrome due to recurrent heterozygous *LMNA* p.T10I mutation. *J Clin Endocrinol Metab.* 2018;103(3):1005-1014. [[PMC free article](#)] [[PubMed](#)] [[Google Scholar](#)]
10. Thong KM, Xu Y, Cook J, et al. . Cosegregation of focal segmental glomerulosclerosis in a family with familial partial lipodystrophy due to a mutation in *LMNA*. *Nephron Clin Pract.* 2013;124(1-2):31-37. [[PubMed](#)] [[Google Scholar](#)]
11. Mory PB, Crispim F, Freire MB, et al. . Phenotypic diversity in patients with lipodystrophy associated with *LMNA* mutations. *Eur J Endocrinol.* 2012;167(3):423-431. [[PubMed](#)] [[Google Scholar](#)]
12. Akinci B, Onay H, Demir T, et al. . Clinical presentations, metabolic abnormalities and end-organ complications in patients with familial partial lipodystrophy. *Metabolism.* 2017;72:109-119. [[PubMed](#)] [[Google Scholar](#)]
13. van Tintelen JP, Hofstra RM, Katerberg H, et al. ; Working Group on Inherited Cardiac Disorders, line 27/50, Interuniversity Cardiology Institute of The Netherlands High yield of *LMNA* mutations in patients with dilated cardiomyopathy and/or conduction disease referred to cardiogenetics outpatient clinics. *Am Heart J.* 2007;154(6):1130-1139. [[PubMed](#)] [[Google Scholar](#)]
14. Fountas A, Giotaki Z, Dounousi E, et al. . Familial partial lipodystrophy and proteinuric renal disease due to a missense c.1045C > T *LMNA* mutation. *Endocrinol Diabetes Metab Case Rep.* 2017;2017:17-0049. [[PMC free article](#)] [[PubMed](#)] [[Google Scholar](#)]
15. Ajluni N, Meral R, Neidert AH, et al. . Spectrum of disease associated with partial lipodystrophy: lessons from a trial cohort. *Clin Endocrinol (Oxf).* 2017;86(5):698-707. [[PMC free article](#)] [[PubMed](#)] [[Google Scholar](#)]
16. RRID: AB_2136056 https://antibodyregistry.org/AB_2136056.
17. RRID: AB_2136057 https://antibodyregistry.org/AB_2136057.
18. RRID: AB_2756879 https://antibodyregistry.org/AB_2756879.
19. Johansen CT, Dubé JB, Loyzer MN, et al. . LipidSeq: a next-generation clinical resequencing panel for monogenic dyslipidemias. *J Lipid Res.* 2014;55(4):765-772. [[PMC free article](#)] [[PubMed](#)] [[Google Scholar](#)]
20. Patni N, Li X, Adams-Huet B, Vasandani C, Gomez-Diaz RA, Garg A. Regional body fat changes and metabolic complications in children with Dunnigan lipodystrophy-causing *LMNA* variants. *J Clin Endocrinol Metab.* 2019;104(4):1099-1108. [[PMC free article](#)] [[PubMed](#)] [[Google Scholar](#)]
21. Sargolzaeiaval F, Zhang J, Schleit J, et al. . *CTCI* mutations in a Brazilian family with progeroid features and recurrent bone fractures. *Mol Genet Genomic Med.* 2018;6(6):1148-1156. [[PMC free article](#)] [[PubMed](#)] [[Google Scholar](#)]

22. RRID: AB_10991536 https://antibodyregistry.org/AB_10991536.
23. RRID: AB_2687626 https://antibodyregistry.org/AB_2687626.
24. RRID: AB_2536381 https://scicrunch.org/resolver/AB_2536381.
25. RRID: AB_2857920 https://antibodyregistry.org/AB_2857920.
26. RRID: AB_2534108 https://scicrunch.org/resolver/AB_2534108.
27. Jackson AS, Pollock ML, Ward A. Generalized equations for predicting body density of women. *Med Sci Sports Exerc.* 1980;12(3):175-181. [[PubMed](#)] [[Google Scholar](#)]
28. Jackson AS, Pollock ML. Generalized equations for predicting body density of men. *Br J Nutr.* 1978;40(3):497-504. [[PubMed](#)] [[Google Scholar](#)]
29. Garg A. Gender differences in the prevalence of metabolic complications in familial partial lipodystrophy (Dunnigan variety). *J Clin Endocrinol Metab.* 2000;85(5):1776-1782. [[PubMed](#)] [[Google Scholar](#)]
30. Simha V, Garg A. Body fat distribution and metabolic derangements in patients with familial partial lipodystrophy associated with mandibuloacral dysplasia. *J Clin Endocrinol Metab.* 2002;87(2):776-785. [[PubMed](#)] [[Google Scholar](#)]
31. Agarwal AK, Zhou XJ, Hall RK, et al. . Focal segmental glomerulosclerosis in patients with mandibuloacral dysplasia owing to ZMPSTE24 deficiency. *J Investig Med.* 2006;54(4):208-213. [[PubMed](#)] [[Google Scholar](#)]
32. Xiong HY, Alipanahi B, Lee LJ, et al. . RNA splicing. The human splicing code reveals new insights into the genetic determinants of disease. *Science.* 2015;347(6218):1254806. [[PMC free article](#)] [[PubMed](#)] [[Google Scholar](#)]
33. Wang M, Marín A. Characterization and prediction of alternative splice sites. *Gene.* 2006;366(2):219-227. [[PubMed](#)] [[Google Scholar](#)]
34. Glynn MW, Glover TW. Incomplete processing of mutant lamin A in Hutchinson-Gilford progeria leads to nuclear abnormalities, which are reversed by farnesyltransferase inhibition. *Hum Mol Genet.* 2005;14(20):2959-2969. [[PubMed](#)] [[Google Scholar](#)]
35. Toth JI, Yang SH, Qiao X, et al. . Blocking protein farnesyltransferase improves nuclear shape in fibroblasts from humans with progeroid syndromes. *Proc Natl Acad Sci U S A.* 2005;102(36):12873-12878. [[PMC free article](#)] [[PubMed](#)] [[Google Scholar](#)]
36. Ben Yaou R, Navarro C, Quijano-Roy S, et al. . Type B mandibuloacral dysplasia with congenital myopathy due to homozygous ZMPSTE24 missense mutation. *Eur J Hum Genet.* 2011;19(6):647-654. [[PMC free article](#)] [[PubMed](#)] [[Google Scholar](#)]
37. Camozzi D, D'Apice MR, Schena E, et al. . Altered chromatin organization and SUN2 localization in mandibuloacral dysplasia are rescued by drug treatment. *Histochem Cell Biol.* 2012;138(4):643-651. [[PMC free article](#)] [[PubMed](#)] [[Google Scholar](#)]
38. Perovanovic J, Hoffman EP. Mechanisms of allelic and clinical heterogeneity of lamin A/C phenotypes. *Physiol Genomics.* 2018;50(9):694-704. [[PMC free article](#)] [[PubMed](#)] [[Google Scholar](#)]
39. Zahr HC, Jaalouk DE. Exploring the crosstalk between *LMNA* and splicing machinery gene mutations in dilated cardiomyopathy. *Front Genet.* 2018;9:231. [[PMC free article](#)] [[PubMed](#)] [[Google Scholar](#)]

